New Horizons in Earth Reinforcement – Otani, Miyata & Mukunoki (eds)
© 2008 Taylor & Francis Group, London, ISBN 978-0-415-45775-0

Analysis of geofiber reinforced soils

A.T. Sway (T. Swe)
HSA Engineers and Scientists, Tampa, FL, USA

S. Bang
South Dakota School of Mines and Technology, Rapid City, SD, USA

ABSTRACT: Various types, shapes, and amounts of geofibers mixed with sand and clay were tested and analyzed in this study. Sixty-six consolidated undrained triaxial compression tests were run and multivariate regression analyses were carried out to obtain the stress-strain relationships. The confining pressure was found to be the most influential parameter. As for the fiber properties, the fiber dosage had greater influence than the fiber aspect ratio. In addition, a finite element analysis program was developed to analyze the behaviors of the geofiber-reinforced soil as a sub-base in a highway system. Analyses indicate that the fibrillated geofiber reinforcement can improve the soil strength better than the tape geofiber reinforcement, but the tape geofiber reinforcement provides more consistent behaviors than the fibrillated geofiber reinforcement.

1 INTRODUCTION

The use of geofibers for reinforcing earth masses has been implemented with great success in recent years. Geofibers consist of relatively small fiber inclusions, such as the polypropylene, distributed randomly as an additive throughout the soil mass (Figure 1). Therefore, the geofiber may be classified as a micro-reinforcement. Unlike traditional macro-reinforcements, such as the Reinforced Earth, the soil nail walls, geofabrics, and geogrids, the geofibers have no preferred orientation, i.e., the material orthotropy does not exist. Therefore, the geofiber-reinforced soil mass can be treated as an isotropic continuum with material properties influenced by the addition of geofibers (Swe et al. 2000). Furthermore, one of the main advantages of using geofibers is the maintenance of the strength isotropy and the absence of potential planes of weakness that can develop parallel to the oriented reinforcements (Gray & Maher 1989, Maher 1988).

The mechanism of the soil strength increase associated with the geofiber-reinforced soils includes: (1) the pullout resistance due to the friction between the individual fiber and the surrounding soil; (2) the adhesion between the individual geofiber and the surrounding soil (in cohesive soils); (3) the micro-bearing capacity of the soil mobilized by the pullout resistance of individual fibers looped across the shear plane; and (4) the increased localized normal stress in the soil across the shear surface resulting from the pullout resistance of the geofibers during shearing of the soil (Gregory & Chill 1998).

Figure 1. Field-mixed geofiber-reinforced soil.

Numerous studies have been conducted in the past to investigate the effects of natural and synthetic fibers on the improvement of the soil shear strength, on the constitutive relationship, and on others through CBR tests on cohesive soils (Hoare 1977, Setty & Rao 1987, Setty & Murthy 1990), direct shear tests on cohesive soils (Gregory & Chill 1998) and cohesionless soils (Gray & Ohashi 1983, Shewbridge & Sitar 1989), triaxial tests on cohesive soils (Gregory & Chill 1998) and cohesionless soils (Gray & Al-Refeai 1986, Setty & Rao 1987, Setty & Murthy 1990), unconfined compression tests on cohesionless soils (Santoni et al. 2001), laboratory model earth

walls (Arenicz & Chowdhury 1988), and strength tests on fly-ash soil (Karniraj & Havanagi 2001). They indicate various degrees of effects of the fiber length, fiber diameter, fiber dosage, fiber aspect ratio, and confining pressure. In addition, Shewbridge & Sitar (1990) developed a closed form solution for determining the development of tension in soil reinforcements from their direct shear tests. Their model accounted for the plastic work to deform the soil and the elastic work to deform the reinforcements in tension and bending. They concluded that the mobilization of tension in the reinforcements was a function of the reinforcement properties and the deformation characteristics of the reinforced soil. They also stated that the relationship between the strength increase of the reinforced soil and the percentage reinforcement was non-linear.

The main objectives of this study are to determine the constitutive relationship of the geofiber-reinforced soils and to investigate the effects of various geofiber properties through an application of geofiber-reinforced soils as a sub-base material in highway construction.

2 MATERIALS AND LABORATORY TESTS

The geofibers used in this study are the fibrillated polypropylene (FIBERGRIDS, 0.034 KN/m^3) and the tape polypropylene. Both are manufactured by the Synthetic Industries, Chattanooga, Tennessee, and they are 2.54 to 5.08 cm in nominal length. These geofibers can be classified as ASTM- D 4101-group1/class1/grade 2. They have a specific gravity of 0.91. The geofibers have a carbon content (ASTM-D1603) of 0.6%, tensile strength (ASTM- D 2256) of 275.8 MPa minimum, tensile elongation (ASTM-D2256) of 25% maximum, and Young's modulus (ASTM-D2101) of 4.19 GPa minimum. They have a coefficient of friction of 0.6 to 0.8 of the tangent friction angle of the soil. The amounts of fibers added into the soil (fiber dosage) were 0.2% and 0.4% by the soil dry unit weight.

Consolidated Undrained (CU) triaxial compression tests with the pore water pressure measurement were conducted for this study. Entire tests were performed at the A.G.T laboratory of the Synthetic Industries. Specimens with a diameter of 7.29 cm and a length of 14.73 cm were tested. The details of the sample preparation methods are well described in reference (Gregory 1996).

A total of 66 triaxial tests were run, including 19 tests conducted with lean clay (CL) samples and 47 tests conducted with poorly graded sand (SP) samples. The lean clay samples have a liquid limit of 26, plastic limit of 14, plasticity index of 12, effective friction angle of 13°, effective cohesion of 21.64 KPa, and dry density of 17.67 KN/m^3. The samples also have a moisture content of 12.9% and the percentage of particles passing number 200 sieve is 55%. The sand properties include an effective friction angle of 33°, moisture content of 10%, and dry density of 15.66 KN/m^3. The specific gravities for clay and sand samples were assumed as 2.7 and 2.65, respectively.

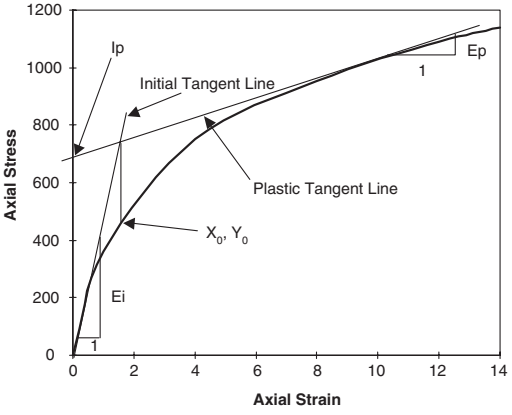

Figure 2. Bilinear parameters.

Confining pressures of 68.95 KPa, 137.89 KPa, and 275.79 KPa were applied to the clay samples. Reduced confining pressures of 34.47 KPa, 68.95 KPa, and 137.89 KPa were, however, used for the sand samples.

3 BILINEAR PARAMETERS

From the observation of the triaxial test data for the geofiber-reinforced soils, it was concluded that the stress-strain relationship follows a bilinear pattern, i.e., a steep initial elastic behavior followed by a relatively flat plastic response. Figure 2 shows the bilinear curve used to simulate the triaxial test results. As described in the figure, five bilinear parameters; the initial tangent modulus Ei, the plastic tangent modulus Ep, the intersection of the axial stress axis and the plastic tangent line Ip, the strain value at the intersection of initial and plastic tangent lines X_0, and the corresponding stress value Y_0, can completely describe the bilinear stress-strain relationship. The value of X_0 can however be determined analytically from Ei, Ep and Ip.

Bilinear parameters were graphically obtained from the CU triaxial test results. For the clay samples, three tests were conducted with unreinforced samples and 16 tests were conducted with fibrillated and tape geofiber-reinforced samples. For the sand samples, three tests were conducted with unreinforced and 20 and 24 tests were conducted with the fibrillated and tape geofiber-reinforced samples, respectively. Three geofiber dosages, 0%, 0.2%, and 0.4%, were applied to both clay and sand samples. Three aspect ratios (length to width ratio) of 0, 8, and 43 were used for the clay

samples and five aspect ratios of 0, 8, 15, 21, and 43 were used for the sand samples. Please note that the zero dosage and zero aspect ratio indicate that the soil samples are unreinforced.

4 LABORATORY TEST RESULTS

Complete laboratory triaxial test results on all 66 samples with different fiber types, fiber widths, fiber dosages, fiber aspect ratios, and confining pressures can be found in reference (Swe 2002).

From the careful observation of the stress-strain curves of the geofiber-reinforced soils, it was observed that they experienced the strain-hardening behavior.

Variations of the bilinear parameters were obtained with respect to three parameters, i.e., the confining pressure, the fiber dosage, and the fiber aspect ratio. It was observed that the values of all bilinear parameters for all samples increased with respect to the increase in these parameters. Among these three parameters, the confining pressure was recognized by far most influential, which was followed by the fiber dosage.

The geofibers tend to slip during deformation at confining pressures below the threshold value or the "critical confining pressure." Above the critical confining pressure, they either yield or break. To reach the critical confining pressure with a typical fiber aspect ratio and fiber dosage, an extremely high overburden pressure would be required. However, the results suggest that the confining pressures used in this study are below the threshold value. Therefore, it can be concluded that the failure mechanism of the geofiber-reinforced soils, under virtually all practical conditions, will be the pullout of the geofibers (Gregory 1999).

5 CONSTITUTIVE RELATIONSHIP

To establish relationships among the bilinear parameters and the fiber dosage, the fiber aspect ratio, and the confining pressure; multivariate regression analyses were carried out on the bilinear parameters obtained from the triaxial test results. The following relationships were assumed based on their observed variations:

$$\begin{aligned} E_i &= a_1 e^{a_2\beta + a_3\alpha + a_4\sigma_3} \\ E_p &= b_1 e^{b_2\beta + b_3\alpha + b_4\sigma_3} \\ I_p &= c_1 e^{c_2\beta + c_3\alpha + c_4\sigma_3} \\ Y_o &= d_1 e^{d_2\beta + d_3\alpha + d_4\sigma_3} \end{aligned} \quad (1)$$

where a_1 through d_4 = coefficients; β = fiber dosage in percentage by the soil dry unit weight; α = fiber aspect ratio (length to width) and σ_3 = confining pressure in KPa. The values of E_i, E_p, I_p, and Y_o are in KPa.

Table 1 shows the optimized values of the coefficients a_1 through d_4.

The bilinear relationship describes the transition of the stress-strain variation, i.e., the initial tangent modulus, the plastic modulus as the asymptote, and the intercept of the asymptote with the ordinate, with the following boundary conditions.

1. At $\varepsilon = 0$, the slope, i.e., the tangent modulus, $\left(\frac{\partial\sigma}{\partial\varepsilon}\right)$ should be equal to the initial modulus;
2. At $\varepsilon = \infty$, the slope should be equal to the plastic modulus and
3. At $\varepsilon = X_0$, the calculated stress should be equal to Y_0.

The following equation describes the bilinear relationship with a smooth transition between elastic and plastic portions and also satisfies the required boundary conditions (Cho 1992, Preber et al. 1995):

$$\sigma = (Ip + Ep\varepsilon)\left[1 - \exp\left(-C\varepsilon^2 \frac{Ei\varepsilon}{Ip}\right)\right]$$

where (2)

$$C = -\frac{Ei}{Ip\,X_0} - \frac{1}{X_0^2}\ln\left[1 - \frac{Y_0}{Ip + EpX_0}\right]$$

ε =axial strain
σ=axial stress

Figure 3 shows a comparison of the stress-strain relationships between the measured and the predicted from Equation 2 for three soil samples reinforced with tape fibers with the fiber dosage of 0.2 %, the aspect ratio of 42, and the confining pressures of 68.95 KPa, 137.89 KPa, and 275.79 KPa.

Table 1. Values of coefficients defined in Equation 1.

	Clay, fibrillated	Clay, taped	Sand, fibrillated	Sand, taped
a_1	6649.881	7858.875	4501.105	2721.757
a_2	2.248218	1.724888	1.279834	2.466681
a_3	0.002291	0.000533	0.002393	0.004825
a_4	0.0046372	0.004407	0.010610	0.012907
b_1	80.72060	80.22342	130.9817	69.68024
b_2	0.597407	0.566442	3.210653	3.750844
b_3	0.005283	0.006299	0.008667	0.099270
b_4	0.005890	0.005806	0.008960	0.010756
c_1	39.81462	40.39581	93.27565	68.49521
c_2	0.328688	0.604583	1.174416	1.125804
c_3	0.000516	1.801e-11	0.003862	0.005238
c_4	0.004699	0.004469	0.008375	0.010631
d_1	29.50490	31.93911	95.23840	65.33820
d_2	0.002854	0.290047	0.774288	0.877247
d_3	0.001247	7.951e-12	0.003688	0.004097
d_4	0.004616	0.004449	0.006850	0.008835

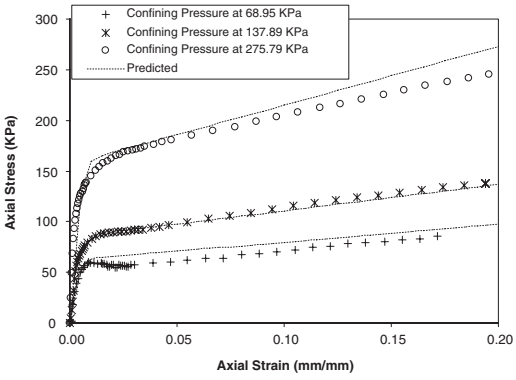

Figure 3. Raw and predicted stress-strain curves for the clay reinforced with tape geofiber.

The tangent modulus of a geofiber-reinforced soil can be obtained by differentiating σ in Equation 2 with respect to ε.

6 FINITE ELEMENT ANALYSIS

A two-dimensional plane strain finite element analysis software for the geofiber-reinforced soils was written to investigate a typical highway cross-section. The program can analyzes the behavior of the soil by three different models: the linear elastic model, the nonlinear hyperbolic model (Duncan et al. 1980) and the bilinear model as described above.

The highway system cross-section considered in this study is a typical interstate freeway system that was provided by the South Dakota Department of Transportation. The cross-section consists of a rigid pavement layer having 7.31 m in width and 0.20 m in thickness of continuously reinforced Portland cement concrete. It has a 3.05 m wide shoulder next to the pavement. The highway system also includes base and sub-base courses with variable thicknesses.

The finite element mesh used for the analysis includes the widths of the pavement of 7.31 m, the shoulder of 3.05 m, the base course of 17.07 m, the sub-base of 31.70 m and the subgrade of 34.75 m. The thickness of the pavement layer was 0.20 m, whereas those of the base and the sub-base were 0.41 m and 1.22 m, respectively. In this study, two different thicknesses of 0.46 m and 0.61 m of the sub-base were used.

The design point load was calculated based on the American Association of State Highway and Transportation Officials' Load and Resistance Factor Design (LRFD) specifications, proposed by Nowak et al. (1993) and Nowak (1999), which increases the design truck loading by combining the standard truck HS20-44 load with a lane load of 472 KN/m.

Three cases were studied: Case 1, fibrillated and tape geofiber-reinforced clay as the sub-base with a clay subgrade; Case 2, fibrillated geofiber-reinforced sand as the sub-base with a sand subgrade; and Case 3, tape geofiber-reinforced sand as the sub-base with a sand subgrade.

Linear elastic constitutive model was used for the pavement and the hyperbolic model was used for the base and the subgrade elements. Bilinear model was applied to the geofiber-reinforced sub-base elements. For fiber reinforced sub-base, the following variables were used: (1) soil: clay and sand, (2) fiber dosage: 0.2% and 0.4%, (3) fiber aspect ratio: 8, 15, 21, and 43, and (4) sub-base thickness: 0.46 and 0.61 m. Following soil material input parameters were used for the analysis:

Pavement: linear, $E = 27.58$ GPa, $\gamma = 23.56$ KN/m^3, $\upsilon = 0.3$
Base: hyperbolic, $k = 600$, $n = 0.4$, $R_f = 0.7$, $C = 0$, $\phi_0 = 42°$, $\Delta\phi = 9°$, $k_b = 175$, $m = 0.2$

Sub-base: Bilinear
Clay subgrade: hyperbolic, $k = 90$, $n = 0.45$, $R_f = 0.7$, $C = 9.57$ KPa, $\phi_0 = 30°$, $\Delta\phi = 0°$, $k_b = 80$, $m = 0.2$
Sand subgrade: hyperbolic, $k = 200$, $n = 0.4$, $R_f = 0.7$, $C = 0$, $\phi_0 = 33°$, $\Delta\phi = 3°$, $k_b = 50$, $m = 0.2$

where γ = unit weight, υ = Poisson's ratio, E = Young's modulus, k = loading modulus, n=loading modulus exponent, R_f = failure ratio, C = cohesion, ϕ_0 = initial friction angle, $\Delta\phi$ = increment in friction angle over 10 fold increase in confining pressure, k_b = bulk modulus, m = bulk modulus exponent.

Twelve runs were completed for Case 1. Fourteen and 16 analysis runs were completed for Cases 2 and 3, respectively. The results of the surface deflection, the vertical displacement, and the maximum compression were investigated and discussed below.

6.1 *Effect of fiber dosage*

Both the fibrillated and tape fibers exhibit similar patterns for the maximum vertical displacement distribution. However, a detailed inspection suggests that the tape geofiber-reinforced sub-base is generally stronger than the fibrillated one.

For surface deflections, in all cases, the lesser values are associated with the thicker sub-base. For all cases, the smallest surface deflection is observed when the sub-base is reinforced with the fiber dosage of 0.4 % and the aspect ratio of 43, which corresponds to the largest amounts of the fiber dosage in this study. With the clay sub-base, increasing the sub-base thickness yields significantly smaller values of the surface deflection. The effects of the fiber dosage and the aspect ratio are not distinctly observed with

the clay sub-base, although they exhibit some visible differences. Maximum surface deflection of 1.26 cm is noted in Case 1. However, the effect of the fiber dosage can be clearly seen with the sand sub-base. This effect is more pronounced with the fibrillated geofiber-reinforced sub-base. For Case 3, for both sub-base thicknesses, only negligible differences are observed with the fiber dosage of 0.2%. Maximum surface deflections of 0.97 cm and 0.89 cm are observed in Cases 2 and 3, respectively. This suggests that the use of the tape geofiber- reinforced soil as the sub-base can slightly reduce the surface deflections.

For the maximum compressive stress developed within the pavement, all cases indicate that the increase in fiber dosage decreases the maximum compression. Maximum compression changes with respect to the sub-base thickness are more pronounced in Cases 1 and 2 than in Case 3. This suggests that the soil beneath the pavement becomes stronger when the fiber dosage and the sub-base thickness increase.

For maximum compressive stress developed within the sub-base, all cases show that the thickness of the sub-base has little effect on the maximum compression. All cases reveal that the maximum compression increases as the fiber dosage increases.

6.2 *Effect of fiber aspect ratio*

In all cases, as the fiber aspect ratio increases, the maximum compression slowly decreases. The decrease in the sub-base thickness, however, increases the maximum compression significantly. In Case 2, almost identical values of the maximum compression in the sub-base are noted with the thickness of 0.46 m and the fiber dosage of 0.4% when compared to that with the thickness of 0.61 m and the fiber dosage of 0.2%.

For the maximum compressive stress in the sub-base, all cases show that the thickness of the sub-base attributes only a small decrease in maximum compression. As for the effect of the fiber aspect ratio, the maximum compression slightly increases as the aspect ratio increases.

For the maximum compressive stress developed within the subgrade, in all cases, the maximum compression increases as the fiber aspect ratio increases. However, the maximum compression becomes relatively smaller when a 0.61 m sub-base configuration is used.

7 CONCLUSIONS

From the measured stress-strain curves of the geofiber-reinforced soils, it was observed that they revealed a strain-hardening behavior. The stress-strain curves for the samples reinforced with tape geofibers exhibited more consistent behavior in improving the soil strength than those reinforced with fibrillated geofibers. In general, the effect of the fiber dosage is found to be more influential than the effect of the fiber aspect ratio.

It was observed that the values of all bilinear parameters for all samples increased as the confining pressure, the fiber dosage, and the fiber aspect ratio increased. Among these three variables, the confining pressure was recognized as the most influential one, followed by the fiber dosage. Although, it was evidenced that the soil strength improved with respect to the increase in the fiber aspect ratio, the effect was not as well defined as those of the confining pressure and the fiber dosage.

It was clear that the soil strength increased with respect to the increase in the fiber dosage. This was more distinct for the tape geofiber-reinforced clay.

It was observed that tape geofibers increased the clay strength more than fibrillated geofibers. However, for the sand, fibrillated geofibers demonstrated slightly stronger soil strength than tape geofibers.

It was also observed that the clay sub-base reinforced with fibrillated geofibers yielded lesser vertical displacements than the tape geofiber-reinforced sub-base. Even though they experienced more or less the same maximum vertical displacements, contour plots suggested that the tape geofiber-reinforced sub-base exhibited stronger soil strength characteristics than the fibrillated one.

Observation on the maximum compressions indicated that the increase in the sub-base thickness had relatively minor effects, as compared to the increase in the fiber dosage and the aspect ratio.

This study was entirely based on experimental laboratory tests conducted on two types of soils (CL and SP). In the future, studies should consider other types of soils and also use a wider variation of the confining pressure.

The study indicates that the fiber dosage has more significant effects on the soil strength improvement than the fiber aspect ratio. Therefore, tests with more diversified fiber dosages are recommended to be conducted in the future.

Based on the limited number of tests, the fibrillated geofiber reinforcement provides slightly better improvements in soil strength, whereas the tape geofiber reinforcement yields more consistent behaviors. Again, additional tests, including the full-scale field tests with detailed instrumentation, need to be conducted to further generalize the results of this study.

ACKNOWLEDGEMENTS

The authors are grateful for the financial and technical supports provided by Garry Gregory of Gregory Geotechnical and the Synthetic Industries, Chattanooga, Tennessee.

REFERENCES

Arenicz, R.M.& Chowdhury, R. 1988. Mechanics of fiber reinforcement in sand. *Journal of Geotechnical Engineering,* ASCE, 109(3), 335–353.

Cho, Y. 1992. Behavior of Retaining Wall with EPS Blocks as Backfill. MS thesis submitted to the South Dakota School of Mines and Technology.

Duncan, J.M., Byrne, P., Wong, K.S. & Mabry, P. 1980. Strength, stress-strain and bulk modulus parameters for finite element analyses of stresses and movements in soil masses. Report No. UCB/GT/80-01, Department of Civil Engineering, University of California, Berkeley.

Gray, D.H. & Al-Refeai, T. 1986. Behavior of fabric versus fiber-reinforced Sand. *Journal of Geotechnical Engineering.*, ASCE, 122(8), 804–820.

Gray, D.H. & Maher, M.H. 1989. Admixture stabilization of sands with discrete, randomly distributed fibers. *Proceedings of XIIth International Conference On Soil Mechanics And Foundation. Engineering*, Rio de Janeiro, Brazil, 1363–1366.

Gray, D.H. & Ohashi, H. 1983. Mechanics of fiber reinforcement in sand. *Journal of Geotechnical Engineering*., ASCE, 109(3), 335–353.

Gregory, G.H. 1996. Design guide for fiber-reinforced soil slopes, version 1.0. A Design Guide submitted to Synthetic Industries.

Gregory, G.H. 1999. Theoretical shear-strength model of fiber-soil composite. *Proceedings of ASCE Texas Section Spring Meeting*, Longview, Texas.

Gregory, G.H. & Chill, D.S. 1998. Stabilization of earth slopes with fiber reinforcement. *Sixth International Conference on Geosynthetics*, Atlanta, Georgia.

Hoare, D.J. 1977. Laboratory study of granular soils reinforced with randomly oriented discrete fibers. *Proceedings of International Conference. On Use of Fabrics in Geotech*., Paris, France, 1, 47–52.

Karniraj, S R. & Havanagi, V.G. 2001. Behavior of cement-stabilized fiber-reinforced fly ash-soil mixtures. *Journal of Geotechnical Engineering*, ASCE, 127(7), 574–584.

Maher, M.H. 1988. Static and dynamic response of sands reinforced with discrete, randomly distributed fibers," Ph.D. thesis submitted to the University of Michigan.

Nowak, A.S. 1999. Calibration of LRFD Bridge Design Code, *NCHRP Report 368, Transportation Research Board*, Washington, D.C.

Nowak, A.S., Nassif, H. & DeFrain, L. 1993. Effect of Truck Loads on Bridges, *Journal of Transportation Engineering*, ASCE, 119 (6), 853–867

Preber, T., Bang, S., Chung, Y. & Cho, Y. 1995. Behavior of Expanded Polystyrene Blocks, *Transportation Research Record*, No. 1462, pp. 36–46.

Santoni, R.L., Tingie, J.S. & Webster, S. L. 2001. Engineering properties of sand-fiber mixtures for road construction. *Journal of Geotechnical Engineering*, ASCE, 127(3), 258-268.

Setty, K.R.N.S. & Murthy, A.T.A. 1990. Characteristics of fiber reinforced lateritic soil. *IGC* (87) Bangalore, India, 329–333.

Setty, K.R.N.S. & Rao, S.V.G. 1987. Evaluation of geotextile-soil friction. *Indian Geotechnical Journal*, 18(1), 77–105.

Shewbridge, S.E. & Sitar, N. 1989. Deformation characteristics of reinforced sand in direct shear. *Journal of geotechnical Engineering*, ASCE, 115(8), 1134–1147.

Shewbirdge, S.E. & Sitar, N. 1990. Deformation-based model for the reinforced sand. *Journal of geotechnical Engineering*, ASCE, 116(7), 1153–1170.

Swe, T. 2002. Analysis of geofiber reinforced soils with bilinear constitutive relationship, Ph.D. thesis submitted to the South Dakota School of Mines and Technology.

Swe, T, Gregory, G.H. & Bang, S. 2000. Constitutive relationship of geofiber reinforced soils. "*Proceedings of the 35th Symposium on Engineering Geology and Geotechnical Engineering*, Pocatello, Idaho, 250–259.